

Received February 20, 2020, accepted March 7, 2020, date of publication March 19, 2020, date of current version March 31, 2020.

Digital Object Identifier 10.1109/ACCESS.2020.2981867

# Robust and Efficient Integrated Antenna With EBG-DGS Enabled Wide Bandwidth for Wearable Medical Device Applications

ADEL Y. I. ASHYAP<sup>1</sup>, SAMSUL HAIMI BIN DAHLAN<sup>1</sup>,  
ZUHAIIRIAH ZAINAL ABIDIN<sup>1</sup>, (Member, IEEE), MUHAMMAD HASHIM DAHRI<sup>1</sup>,  
HUDA A. MAJID<sup>1</sup>, (Member, IEEE),  
MUHAMMAD RAMLEE KAMARUDIN<sup>1</sup>, (Senior Member, IEEE), SEE KHEE YEE<sup>1</sup>,  
MOHD HAIZAL JAMALUDDIN<sup>2</sup>, (Member, IEEE),  
AKRAM ALOMAINY<sup>3</sup>, (Senior Member, IEEE), AND  
QAMMER H. ABBASI<sup>4</sup>, (Senior Member, IEEE)

<sup>1</sup>Center for Applied Electromagnetics (EMCenter), Faculty of Electrical and Electronic Engineering, Universiti Tun Hussein Onn Malaysia (UTHM), Parit Raja 86400, Malaysia

<sup>2</sup>Wireless Communication Centre, Faculty of Electrical Engineering, Universiti Teknologi Malaysia, Johor Bahru 81310, Malaysia

<sup>3</sup>Antennas and Electromagnetics Research Group, School of Electronic Engineering and Computer Science, Queen Mary University of London, London E1 4NS, U.K.

<sup>4</sup>School of Engineering, University of Glasgow, Glasgow G12 8QQ, U.K.

Corresponding authors: Samsul Haimi Bin Dahlan (samsulh@uthm.edu.my) and Zuhairiah Zainal Abidin (zuhairia@uthm.edu.my)

This work was supported in part by the Center for Applied Electromagnetic (EMCentre), Universiti Tun Hussein Onn Malaysia for supporting this research under Vot No. E15224, and in part by the Ministry of Education Malaysia (MOE) through the Fundamental Research Grant Scheme (FRGS) under Grant VotNo. K186.

**ABSTRACT** A compact wearable symmetrical e-slots antenna operated at 2.4 GHz was proposed for Medical Body Area Network applications. The design was printed onto a highly flexible fabric material. The final design topology was achieved by the integration of symmetrical e-slots antenna with an Electromagnetic Band-Gap (EBG) and Defected Ground Structure (DGS). The use of EBG was to isolate the body and antenna from each other whereas the DGS widened the bandwidth. This combination forms a novel and compact structure that broadens bandwidth. This broadened bandwidth makes the structure robust to deformation and loading in the human body. The design achieved a measured impedance bandwidth of 32.08 %, a gain of 6.45 dBi, a Front to Back Ratio (FBR) of 15.8 dB, an efficiency of 72.3% and a SAR reduction of more than 90%. Hence, the integration of symmetrical e-slots antenna with EBG and etched DGS is a promising candidate for body-worn devices.

**INDEX TERMS** AMC, EBG, metasurface, metamaterial, medical body-area network, SAR, textile antennas, wearable textile.

## I. INTRODUCTION

Nowadays, the requirements of wearable devices in the ICT arena for in-body, off-body, and on-body applications; the Internet of Things, and Wireless Sensor Networks has drawn great concern. Wearable antennas are an essential part of these devices. They are broadly utilized in several applications, such as health-care, sport monitoring, emergency search, physical training, and the military [1]–[5].

The associate editor coordinating the review of this manuscript and approving it for publication was Chan Hwang See<sup>1</sup>.

An essential merit of these antennas is that they required to operate on the human body, making them face more challenges than a traditional antenna. One of the main challenges facing the implementation of wearable antennas is the stable performance of the human body [6], [7].

Unlike traditional antennas, which are generally positioned in free space, wearable antennas are located near human tissues under various deformation conditions. These tissues have a highly dielectric nature, effecting antenna performance parameters such as reflection coefficient ( $S_{11}$ ), bandwidth, gain (dBi), and radiation characteristics [8], [9].

Furthermore, electromagnetic radiation from these antenna needs a Specific Absorption Rate (SAR) level that is within the health and safety limit set by the European Union (EU) of over 10 g and the United States (US) of over 1 g [8], [9].

In order to rectify these problems, EBG structures were introduced to wearable antenna designs to provide a high degree of isolation from the human body [10]. As a result, electromagnetic coupling was alleviated compared to traditional antennas. The SAR level was also dramatically decreased to comply with standards set by ICNIRP and FCC [11] [12]. On the other hand, these structures are either too thick for Medical Body Area Network (MBAN) applications [13]–[19], utilize semi-flexible materials that are not sufficiently deformable and are uncomfortable for users [20], [21] or suffer from low FBR [13], [14], [21]–[26]. Furthermore, most EBG designs suffer from narrow bandwidth [13]–[16], [20]–[25], [27], [28] causing frequency shifts that are sensitive in the vicinity of the human body and during deformation. In order to reduce frequency shift sensitivity during body load and deformation, a large bandwidth is required. Frequency shifts will not have much impact with a large bandwidth, since the desired band would still remain within a –10 dB bandwidth. Furthermore, high-bandwidth is also needed for high data rates and short-range indoor communications [29].

Therefore, to overcome the problem of narrow bandwidth in EBG antenna design, a novel Defected Ground Structure (DGS) was etched on the back of EBG array, disturbing the current distribution in the ground plane. As a result, the bandwidth is widened, which reduces sensitivity to frequency detuning due to load or deformation on the human body. Furthermore, the proposed design has a small volume and provides reasonable gain. In addition, the combination of EBG-DGS is significantly different from previously proposed EBG ground plane backed antennas because it enables a large bandwidth [13]–[16], [20]–[25], [27], [28] and its antenna is compact and superior in performance.

This paper is arranged as follows: Section II discusses the antenna, EBG and DGS designs using CST Microwave Studio software [30]. Section III covers the integration of the antenna alone and over  $2 \times 2$  EBG with and without etched DGS in free space. The effects of bending when the antenna over  $2 \times 2$  EBG with etched DGS is also investigated in this section. Section IV considers the behavior of the antenna alone and with artificial structures when loaded on chests and arms as well as on volunteer males. SAR studies were also performed in this section. Section V concludes with the performance of the proposed design.

## II. ANTENNA, EBG AND DGS DESIGNS

### A. ANTENNA DESIGN

The antenna is constructed on a fabric jeans substrate with a permittivity of 1.7 and a thickness of 0.7 mm. This fabric is selected due to its lightweight and flexibility. The radiating elements are made from Shieldit™ material with a

thickness of 0.17 mm. A Cutter Printer (CAMEO) is used to cut the conducting materials. A novel monopole antenna based on symmetrical e-slots etched on the radiation patch is proposed. The evaluation process of the design is depicted in Fig.1. The substrate is fixed at a width of 20 mm and a length of 30 mm to fit the growth of wearable devices. The ground was fixed at 8.75 mm for all evaluation processes. The impact of introducing e-slots diverted current distribution and enlarged the effective current path length [31]. Hence, the resonant frequency shifted from a higher band to the desired band as presented in Fig.2.

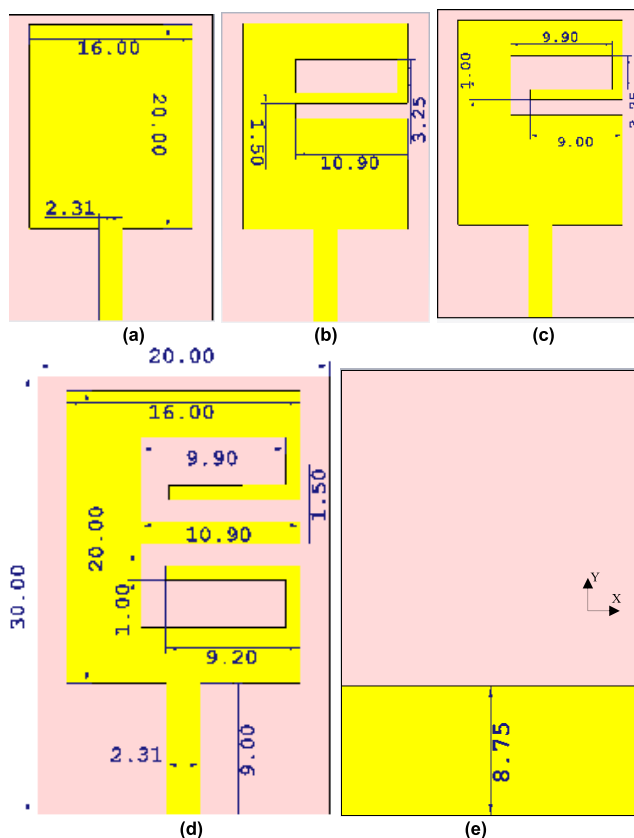


**FIGURE 1.** Proposed design processes: (a) Conventional Patch; (b) slot antenna; (c) e-slot antenna; (d) Final proposed antenna (symmetrical e-slots antenna); and (e) ground plane of all design processes. All dimensions are in mm.

The physical layer of the proposed antenna is modelled as an equivalent circuit based on lumped element components. Generally, conventional monopole antenna is modelled as a simple parallel RLC resonant circuit based on the cavity model revealed in Fig.3 (a). The values of the components R, L, and C were determined by the conventional formulae given in [31], [32].

The adjustable symmetrical e-slots presented on the radiating element were the key parameter that controlled  $S_{11}$ . They altered the current distribution. Hence, two currents flow through the radiating element; one is a normal current that flows in any traditional radiating patch and the other is a meandering current around the e-slots, which

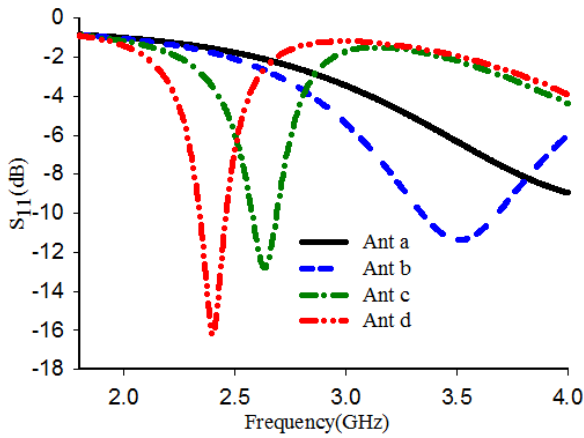


FIGURE 2.  $S_{11}$  based on the evaluation process.

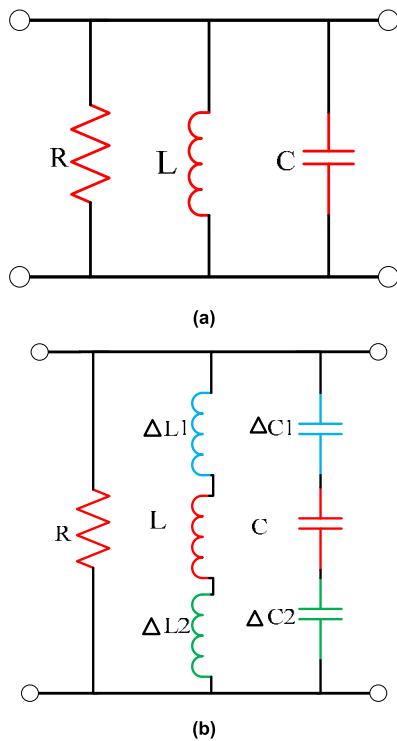


FIGURE 3. Equivalent circuits for: (a) Conventional Patch and (b) Proposed design.

increases the current paths. Therefore, the resonant frequency shifted to a lower band. Each e-slot was modelled as an extra series of inductances and capacitances to the equivalent circuit of the conventional monopole antenna as presented in Fig.3 (b).

The equivalent circuit of the proposed antenna is simulated and optimized using Advanced Design System (ADS) software. The  $S_{11}$  of the equivalent circuit is in line with the result from CST of the physical insight of the monopole antenna based on symmetrical e-slots as revealed in Fig.4. The results from both software were found in close agreement.

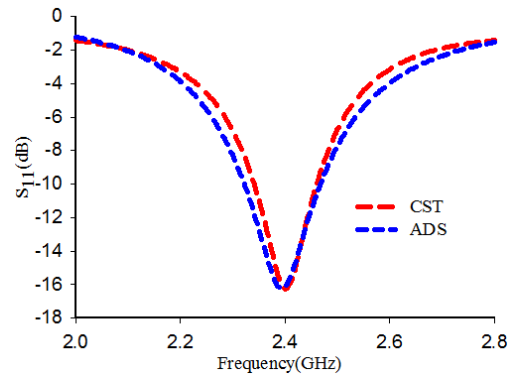


FIGURE 4. Comparison of  $S_{11}$  physical layer and equivalent circuit.

**B. EBG DESIGN**

The presence of vias in EBG designs for wearable applications could be uncomfortable. It also increases the complexity of fabrication [17]. Therefore, vias EBG s is chosen as shown in Fig.5 (a). However, removing via increases structure size because of decreases in effective inductance. Thus, effective inductance should be increased without additional design complexity. Hence, a slot is introduced in the conventional square with dimensions of 22.60 x 22.60 mm<sup>2</sup> as displayed in Fig.5 (b) to form a square loop. This square loop simplifies the fabrication process of this proposed design.

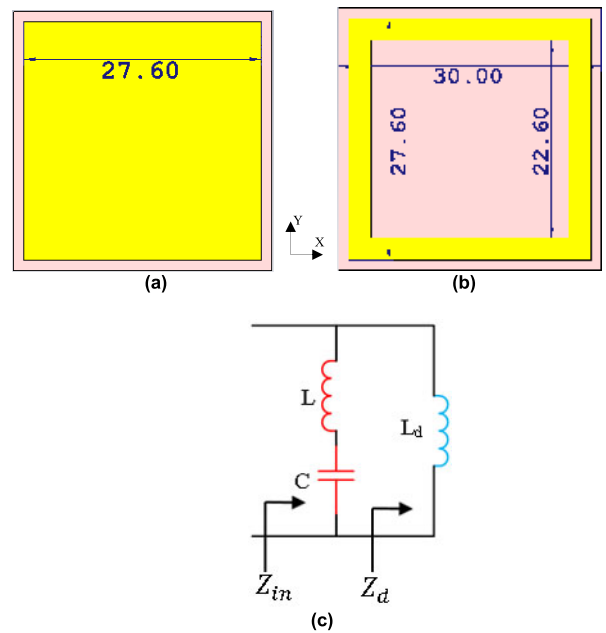


FIGURE 5. EBG unit cell: (a) Conventional square patch; (b) Square loop; and (c) Equivalent circuit model of (b). All dimensions are in mm.

The operational mechanism of the square loop EBG unit cell was clarified by the lumped LC equivalent circuit as shown in Fig.5(c). The capacitance of the surface comes from gaps between adjacent patches and between loops while inductance comes from the loop of the metallic patch.

The values for inductance and capacitance were determined by the following formulas [24], [17]:

$$L = \ell_n \frac{\mu_0}{4\pi} \ln \left\{ 1 + \frac{32h^2}{w_n^2} \left[ 1 + \sqrt{1 + \left( \frac{\pi w_n^2}{8h^2} \right)^2} \right] \right\} \quad (1)$$

where  $\ell$  and  $w$  are the length and width of the strip, respectively, and  $h$  is the substrate thickness

$$C = \frac{W\epsilon_0(1 + \epsilon_r)}{\pi} \cosh^{-1} \left( \frac{W + g}{g} \right) \quad (2)$$

where  $W$  is width of conductive material and  $g$  is the gap size between the two adjacent unit-cells.

$$L_d = \mu_0 h \quad (3)$$

Fig.6 shows a comparison between the square patch with and without a slot of the same dimension. It appears that the square patch and the square loop have a zero-degree resonant frequency at 3.88 GHz and 2.4 GHz, respectively. This proves that by introducing the slot, the effective inductance increased and the volume decreased. Furthermore, the equivalent circuit for the square loop was modelled and optimized by ADS software. It can be seen from Fig.6 that the square loop (physical layer) and equivalent circuit were in agreement.

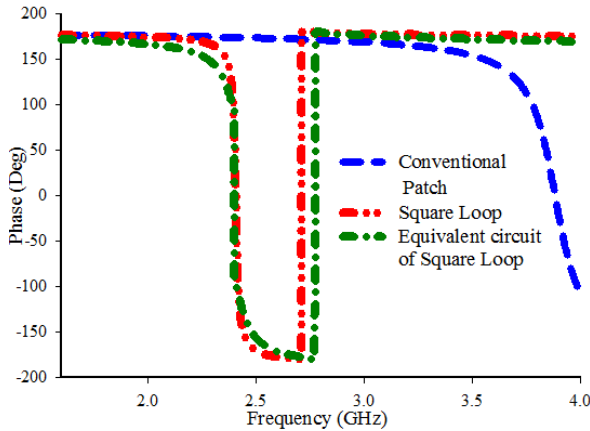


FIGURE 6. Reflection phase of EBG unit cell.

### C. DGS DESIGN

A novel DGS is printed on the same substrate of EBG. The structure is etched on the ground and its characteristics are analyzed using microstrip line on the top of the substrate as displayed in Fig.7. The difference between the conventional dumbbell-shaped DGS [33] and the proposed DGS is that the dumbbell-shape consists of two rectangular slots connected by a slot gap, while the proposed DGS consists of a rectangular slot with five branches, which strongly divert current distribution in the ground plane as displayed in Fig.7 (c) and reduce the Q factor to widen bandwidth [34].

The equivalent circuit of the proposed DGS structure is simplified as a parallel LC resonator as depicted in Fig.8, where the inductance is controlled using etched area size

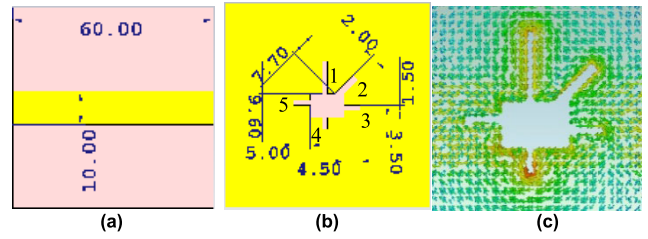


FIGURE 7. Proposed DGS structure; (a) front view; (b) Back view; and (c) Surface current (1-5 indicate slot order). All dimensions are in mm.

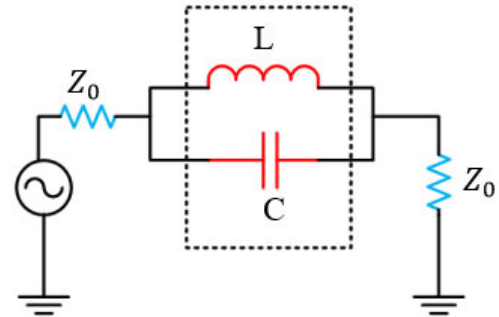


FIGURE 8. Equivalent circuit for the proposed DGS structure.

while capacitance was controlled by the distance between the branch slots. Hence, the etched area is inversely proportional to capacitance and proportional to inductance. As the etched area was increased inductance increased, therefore, lowering the cut-off frequency.

The series reactance value of the equivalent circuit is determined using the prototype element value of the one-pole Butterworth response, which is given in several references [35], [36]. The parallel capacitance value was extracted using attenuation pole location [34]. Finally, Equation (4) and (5) [34] are used to calculate the capacitance and inductance values to fulfil the demands of the Butterworth low-pass response.

$$C = \frac{\omega_c}{Z_{0g_1}} \cdot \frac{1}{\omega_0^2 - \omega_c^2} \quad (4)$$

$$L = \frac{1}{4\pi^2 f_0^2 C} \quad (5)$$

where  $\omega_c$  and  $\omega_0$  is the cutoff and resonance frequencies, respectively, and  $g_1$  is the prototype value of the Butterworth-type low-pass filter.

The characteristic responses of the proposed DGS are based on the Full-Wave Simulator (CST), ADS, and the measurement presented in Fig.9. It showed that the simulated results have discrepancies compared to the measured result. These discrepancies may due to the fabrication tolerance and measuring environment.

### III. PERFORMANCE OF THE ANTENNA OVER EBG AND EBG-DGS IN FREE SPACE

The proposed monopole antenna is based on symmetrical e-slots antenna positioned over  $2 \times 2$  EBG with and

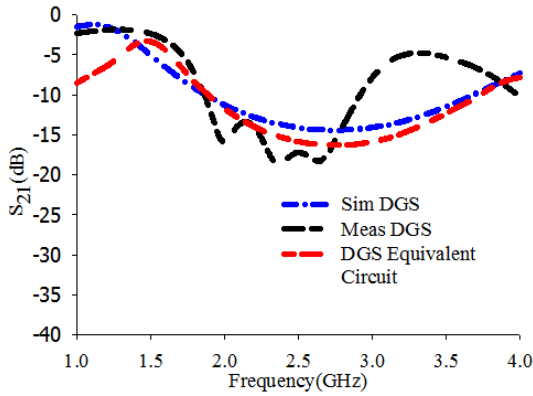


FIGURE 9.  $S_{21}$  of proposed DGS structure.

without DGS structure etching on the EBG ground. The overall dimensions were  $60 \times 60 \times 2.4 \text{ mm}^3$ . A foam 1 mm thick is used as an isolation between the proposed monopole antenna and the EBG structures to avoid short circuits and alleviate mismatches. The characteristics of the foam were  $\epsilon_r = 1.05$  and  $\delta = 0.0003$ .

**A. ANTENNA OVER  $2 \times 2$  EBG WITH AND WITHOUT ETCHED DGS ARRAYS**

Modern wearable systems require a compact design and broad bandwidth to avoid sensitivity to resonant frequencies from deformation and loading on the human body. Therefore, DGS and EBG are introduced in this paper to broaden bandwidth and to act as isolation between the body and antenna, respectively. These two methods are integrated with the antenna to form a compact and robust design that complies with advances in technology.

Placing an antenna on EBG array will detune the resonant frequency [7] because of mutual impedance coupling. Hence the dimension of the antenna is optimized to resonate at 2.4 GHz. Furthermore, introducing DGS to the ground of EBG also detuned  $S_{11}$  due to changes in the current distribution that led to variations in distributed inductance and capacitance. This changed EBG characteristics, requiring the EBG to be optimized to resonate at the desired frequency. The updated antenna and EBG dimensions is depicted in Fig. 10(a). The contribution of each DGS slot branch to bandwidth widening is displayed in Fig. 11.

The S-parameters of the antenna alone and over  $2 \times 2$  EBG array with and without etched DGS are presented in Fig. 12. It is seen that the antenna over the  $2 \times 2$  EBG array with etched DGS have a better reflection coefficient and bandwidth than the antenna alone and antenna over a  $2 \times 2$  EBG array. This could be due to that the novel DGS disturbing current distribution in the ground plane. In addition, it could also be due to a decrease in the surface wave excitation. As the surface wave excitation is alleviated, the Q factor and the stored energy is reduced, which results in bandwidth improvement [34]. This wider bandwidth is useful in wearable antennas because it ensures that the desired frequency band is covered even if

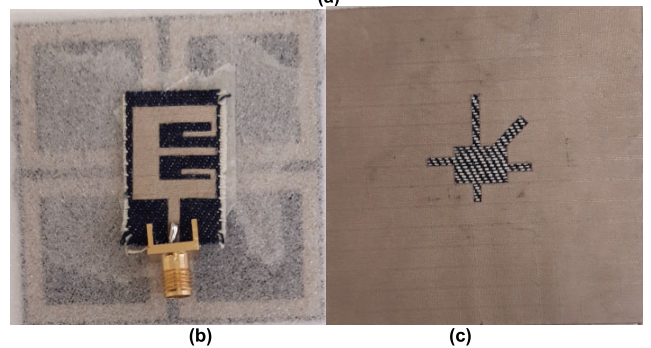
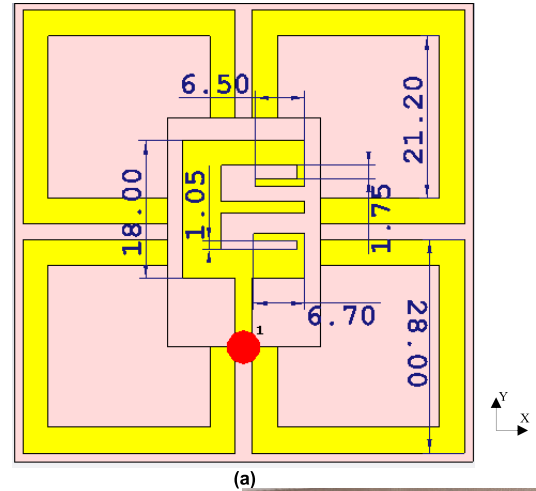


FIGURE 10. (a) Integrated proposed antenna: EBG-DGS; (b) Prototype front view; and (c) Prototype back view.

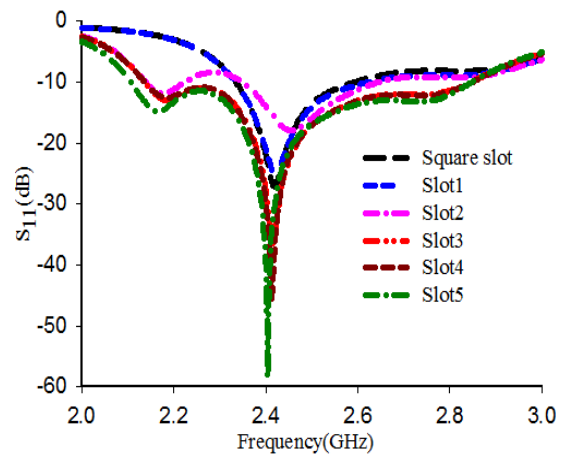
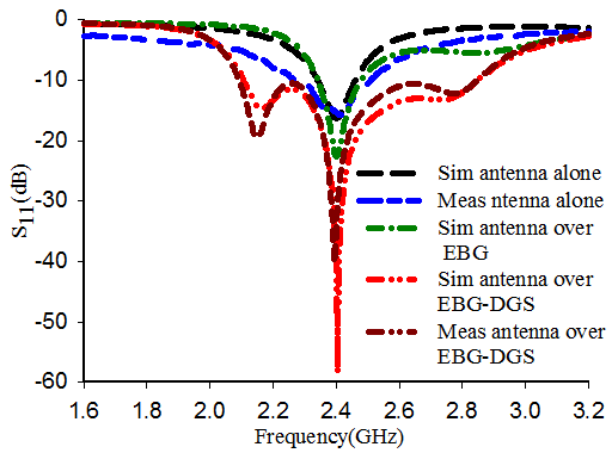


FIGURE 11. Influence of each slot branch on bandwidth.

there is shift due to deformation and loading on the human body.

The measured S-parameters of the antenna alone and antenna over  $2 \times 2$  EBG with etched DGS is illustrated in Fig. 12. It can be observed that the measured results agree with the simulated results with slight discrepancies that could be due to fabrication or soldering errors.

Fig. 13 presents the simulated radiation patterns of the antenna alone and over a  $2 \times 2$  EBG array with and without



**FIGURE 12.** Simulated and measured  $S_{11}$  of the antenna with and without EBG-DGS.

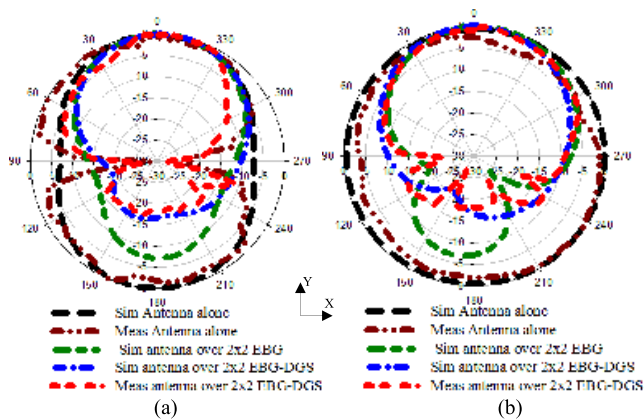


**FIGURE 13.** Radiation pattern of the antenna alone and over  $2 \times 2$  EBG with and without etched DGS (a) E-plane and (b) H-plane.

etched DGS on the E-plane and H-plane. The results illustrate that the symmetrical e-slots antenna had the maximum number of radiation points along  $\pm z$ -direction in its E-plane, and an omnidirectional pattern in its H-plane, indicating major backwards radiation. However, placing the antenna over a  $2 \times 2$  EBG array with and without etched DGS directed maximum radiation to the positive z-direction. The simulated results illustrate that the antenna over a  $2 \times 2$  EBG array improved the FBR by 7 dB and by introducing DGS on the back of EBG FRB further improved from 7 dB to 15.8 dB. The radiation pattern of the antenna over a  $2 \times 2$  EBG array with etched DGS was verified as depicted in Fig.13. The measured results agreed with the simulated results with slight discrepancies that could be due to cable, connector, or fabrication errors. Furthermore, the incorporated antenna-EBG with etched DGS has revealed an efficiency of 72.3%.

**B. IMPACTS OF DEFORMATION ON DESIGN PERFORMANCE**

The above analysis of free space shows that the integrated symmetric e-slots antenna on a  $2 \times 2$  EBG array with etched

DGS had better performance, especially the widening of the bandwidth. Therefore, a further investigation is conducted to evaluate the proposed design when deformed and loaded on a body.

The deformation is conducted to demonstrate its ability to withstand a certain amount of structural bending. Therefore, the proposed integrated design was experimentally validated with several degrees of bending to ensure its conformability before loading onto a human body curvature. The design is measured under four bending scenarios. It was bent around a foam cylinder with a diameter ( $d$ ) of 70 mm, 80 mm, 100 mm, 140 mm along a y-axis, x-axis,  $y+45^\circ$  axis, and  $y-45^\circ$  axis as depicted in Fig.14. These four scenarios gave a clear image of the effect of bending on the design. The diameters are carefully chosen to mimic chest and arm sizes in the human body.

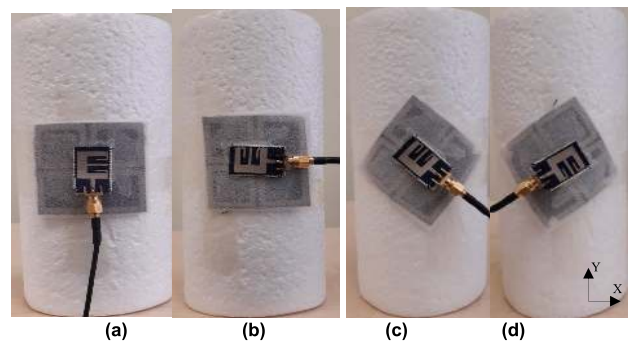


**FIGURE 14.** Bending orientations: (a) y-axis; (b) x-axis; (c)  $y+45^\circ$  axis; and (d)  $y-45^\circ$  axis.

Fig. 15(a-d) provides the  $S_{11}$  measurement results of the four scenarios. It is seen that the  $-10$ -dB impedance bandwidth of 2.4 GHz is maintained in all cases of varying diameters, even at extreme degree of bending  $d = 70$  mm.

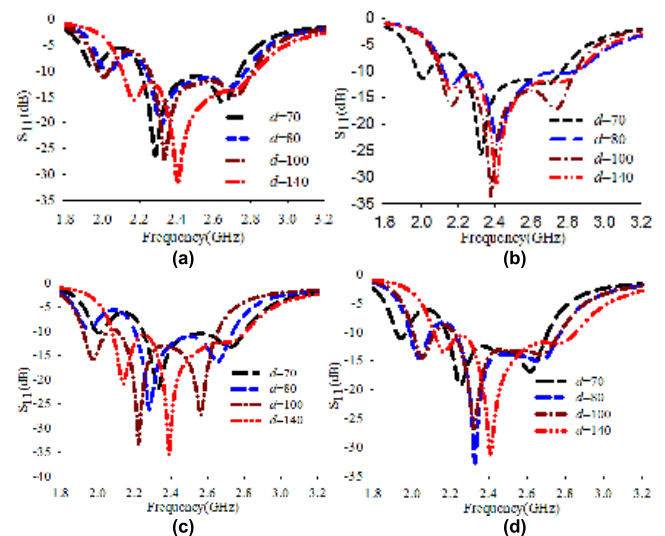


**FIGURE 15.** Performance of the design under bending scenarios; (a) y-axis; (b) x-axis; (c)  $y+45^\circ$  axis; and (d)  $y-45^\circ$  axis.

The frequency shifts do not have much impact, due as the wide bandwidth still covered the desired band. Furthermore, bending along  $y \pm 45^\circ$  has a greater effect than along the y-axis and x-axis, but still maintained the  $-10$  dB bandwidth at the desired band. These effects could be due to bending along the branch slots that disturbed the surface current. Hence, antenna characteristics may change due to variations in inductance and capacitance. This investigation demonstrates that the design is highly conformable and is a good candidate for body-worn devices.

Fig. 16 gives the measured normalized radiation patterns of the antenna over a  $2 \times 2$  EBG array with etched DGS under different bending scenarios. These measurements are carried out along a diameter of 140 mm in four bending scenarios. The design was fixed onto foam using tape. The results revealed that the radiation pattern almost maintained the same shape as the normal scenario (flat) with a reduction in FBR. This reduction was significant for bending along  $y \pm 45^\circ$  due to the effect of branch slots being disturbed, which effected the surface current and radiation pattern. This trend was also realized for the s-parameters. Overall, the design is durable to structural bending in all scenarios.

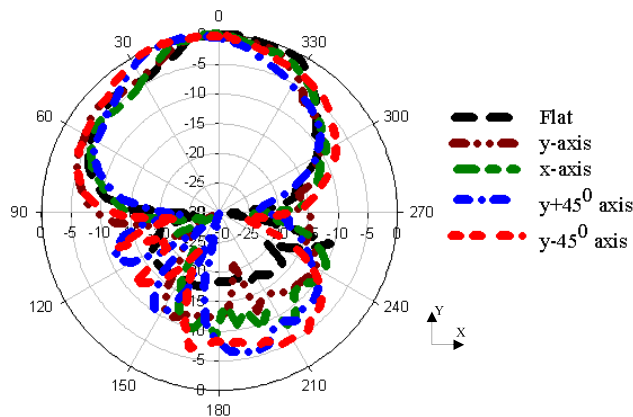


FIGURE 16. Radiation patterns under bending four scenarios at  $d=140$  mm.

#### IV. ANTENNA PERFORMANCE ON BODY

The next investigation of the presented wearable symmetrical e-slots antenna design is to evaluate its performance when loaded onto the human body. Numerical studies are conducted using CST. A multi-layer model tissue is developed to mimic the human body. The chest is mimicked by a cuboid of  $150 \times 150 \times 40$  mm<sup>3</sup> [24], [25] whereas the arm was mimicked by a cylindrical with a diameter of 80 mm and a length of 150 mm as seen in Fig.17 [20]. Each model had four layers with a typical thickness, permittivity, density, conductivity, and mass as tabulated in Table 1 [20], [24]. The chest and arm are chosen to represent normal and deformed cases, respectively.

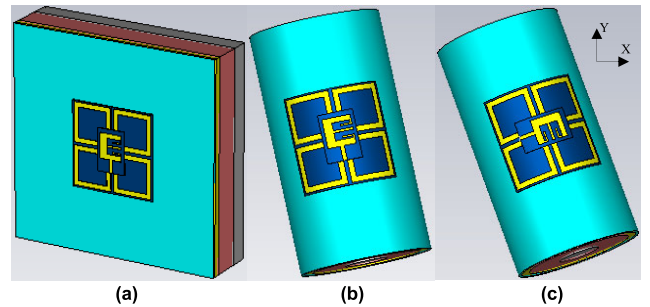


FIGURE 17. Position of the proposed design on the human model: (a) on chest; (b) on arm along y-axis; and (c) on arm along x-axis.

TABLE 1. Properties of multilayer body tissues [20], [24].

	Fat	Muscle	Bone	Skin
Density (kg/m <sup>3</sup> )	900	1006	1008	1001
$\sigma$ (S/m)	0.11	1.77	0.82	1.49
Thickness (mm)	5	20	13	2
$\epsilon_r$	5.27	52.67	18.49	37.95

#### A. PLACED ON CHEST (NORMAL SCENARIO)

The symmetrical e-slots antenna alone and over a  $2 \times 2$  EBG array with etched DGS are positioned on the chest model (normal scenario) to evaluate their performance. Fig.18 shows the simulated result. It can be seen that the  $S_{11}$  of the symmetrical e-slots antenna did not operate in the normal scenario at 2.4 GHz and moved to a lower frequency of 1.4 GHz. Nevertheless, placing antenna over a  $2 \times 2$  EBG array with etched DGS reduced frequency detuning compared to the antenna alone. The desired frequency was still within the  $-10$  dB bandwidth.

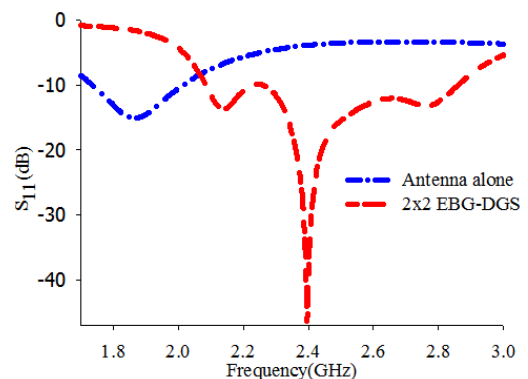
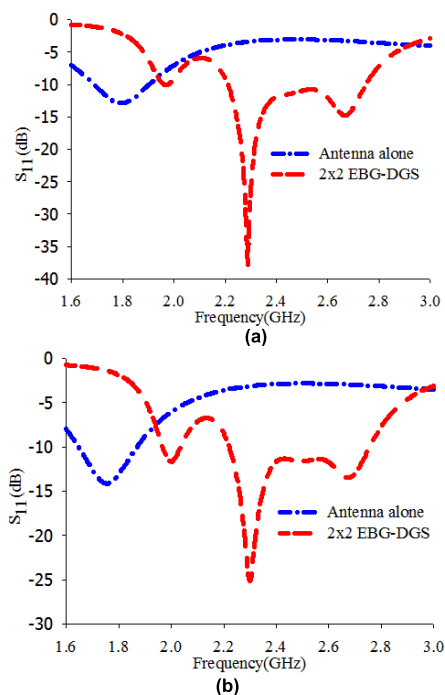


FIGURE 18. Design performance on chest model.

#### B. PLACED ON ARM (DEFORMED SCENARIO)

In this subsection, the impacts of deformation on the arm model was investigated. The designs were placed along the x-axis and y-axis. Fig.19 provides the simulated results. It can



**FIGURE 19.** Design performance on the arm model (a) y-axis and (b) x-axis.

be seen that the symmetrical e-slots antenna had almost the same effect on both planes.  $S_{11}$  resonated at lower frequencies of 1.795 GHz and 1.756 GHz along the y-axis and x-axis respectively. Nonetheless, placing the antenna on a  $2 \times 2$  EBG array with etched DGS alleviated shifts in  $S_{11}$  compared to the antenna alone. However, even there is a shift in the resonant frequency, but due to wide bandwidth the desired band still covered along both axes.

It can be concluded that resonant frequency in all cases was affected by the highly dielectric nature of human body tissues, but introducing EBG with etched DGS has reduced affect. This is due to EBG acting as insulation between the antenna and body, while etching DGS had broadened the design bandwidth, making the design more sustainable on all body curvatures. Hence, antenna over  $2 \times 2$  EBG array with etched DGS structure is a good candidate for body-worn systems.

**C. RADIATION PATTERN PERFORMANCE ON BODY**

A full-wave simulation was conducted to assess the radiation pattern of symmetrical e-slots antenna alone and over a  $2 \times 2$  EBG array with etched DGS. The assessment is based on a normal case (chest) and bend cases along the x-axis and y-axis (arm). Fig.20 provides the result of these cases. When the antenna was without EBG-DGS, it observed that the radiation is significantly affected and became more directive. FBR increased, indicating that the body absorbed power by around 9 dB. As a result, all radiated powers become very weak. However, placing antenna over  $2 \times 2$  EBG array with etched DGS revealed more stable radiation patterns.

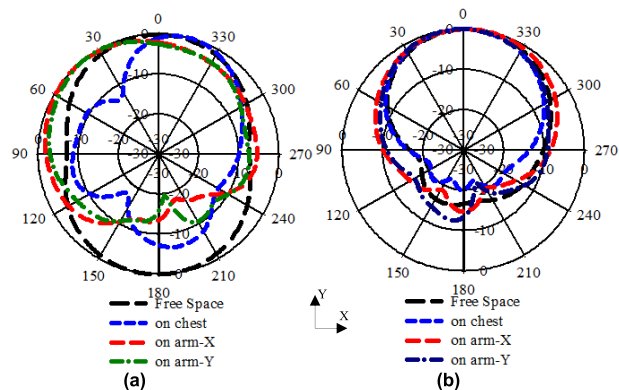


**FIGURE 20.** Radiation performance on body: (a) Antenna alone; (b); and (b) Antenna over  $2 \times 2$  EBG with etched DGS.

The results also show comparable radiation pattern between free space and body loading. Overall, the increment of FBR when loaded on the body, especially when the antenna was alone, is due to the high permittivity of the body compared to the substrate antenna material.

**D. EXPERIMENTAL RESULT ON REAL HUMAN BODY**

The proposed antenna over  $2 \times 2$  EBG array with etched DGS was validated on different parts of a real male volunteer. The volunteer had a weight of 78 kg and a height of 160 cm. The design was positioned directly on the arm along the y-axis and x-axis, on the chest and back, and on jeans on the leg and thigh as seen in Fig. 21.

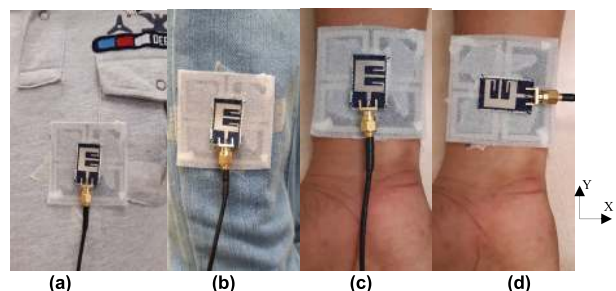


**FIGURE 21.** Position of antenna with EBG-DGS at several parts of real male volunteer: (a) chest; (b) thigh; (c) arm-Y; and (d) arm-X.

In order to show the usefulness of introducing EBG-DGS, the comparison results of the antenna with and without EBG etched DGS when placed on a body and in free space are plotted in Fig. 22. It observed that the symmetrical e-slots antenna placed at several positions on the volunteer did not operate at the desired frequency of 2.4 GHz as seen in Fig.22 (a). The antenna tended to operate at lower frequencies due to the highly dielectric nature of human tissue. While Fig.22 (b) provides the measured results for the antenna over a  $2 \times 2$  EBG array with etched DGS. It can be seen that the  $-10$  dB bandwidth covered the desired frequency of 2.4 GHz. The slight shifted of  $S_{11}$  has no impact on the design due to its wide bandwidth. The bandwidth range is not greatly affected



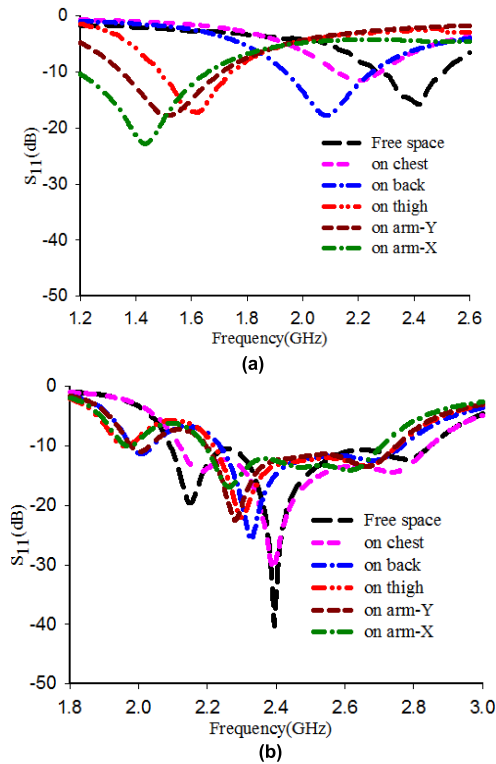


FIGURE 22. Performance of the proposed design on several parts of a volunteer male: (a) antenna alone and (b) antenna with EBG-DGS.

TABLE 2. SAR evaluation of antenna without metasurface (unit: W/kg).

Distance from the phantom (mm)	Antenna without EBG-DGS					
	chest		Arm-Y		Arm-x	
	1 g	10 g	1 g	10 g	1 g	10 g
2	5.3	2.36	6.46	2.69	6.78	3.06
4	4.75	2.22	5.9	2.53	6.16	2.81
6	4.04	1.99	5.03	2.29	5.23	2.5
8	3.35	1.73	4.16	1.99	4.27	2.15

and was similar to the free space measurements. The introduced EBG-DGS shows the usefulness of isolating antenna from the human body and widening bandwidth.

E. SAR EVALUATION

The safety evaluation of the symmetrical e-slots antenna over a 2 × 2 EBG array with etched DGS operating over a human body was carried out to ensure that the SAR level comply the safety limits. The evaluation is based on the regulatory standards given by the FCC and ICNIRP of a maximum level of 1.6 W/kg for an average of more than 1 gram of tissue and 2 W/kg for an average of more than 10 grams of tissue. The same models used to evaluate the performance of the design in section IV were used for SAR assessment.

In this study, the IEEE C95.1 standard provided in CST was used for SAR assessment at 2.4 GHz with an input power of 100 mW. The design was evaluated at several distances (2, 4, 6, and 8 mm) from the model under both a normal scenario (chest) and bent scenario (arm) along the x-axis and

TABLE 3. SAR evaluation of antenna with metasurface (unit: W/kg).

Distance from the phantom (mm)	Antenna with EBG-DGS					
	chest		Arm-Y		Arm-x	
	1 g	10 g	1 g	10 g	1 g	10 g
2	0.983	0.258	0.374	0.108	0.321	0.01
4	0.49	0.15	0.194	0.054	0.122	0.041
6	0.272	0.095	0.112	0.031	0.08	0.026
8	0.166	0.063	0.062	0.021	0.032	0.013

y-axis. The results are presented in Table 2 and Table 3 for the antenna alone and antenna over EBG with etched DGS, respectively. The result revealed that when the antenna is alone SAR values do not comply with the standards even when the design is placed 8 mm away from the model. However, adding EBG with etched DGS to the antenna brought SAR values far below the safe level of 1.6 W/kg under the FCC average and 2 W/kg under the ICNIRP average even when the design is placed 2 mm away from the model. It was seen that as the design was placed further from the model, the SAR values dramatically decreased. Overall, the EBG with etched DGS reduced SAR by more than 90%. Fig.23 reveals the SAR values 4 mm away from the model over 1 g average tissue. Unfortunately, due to the unavailability of the SAR measurement equipment, the simulated results could not be compared with the measurement results.

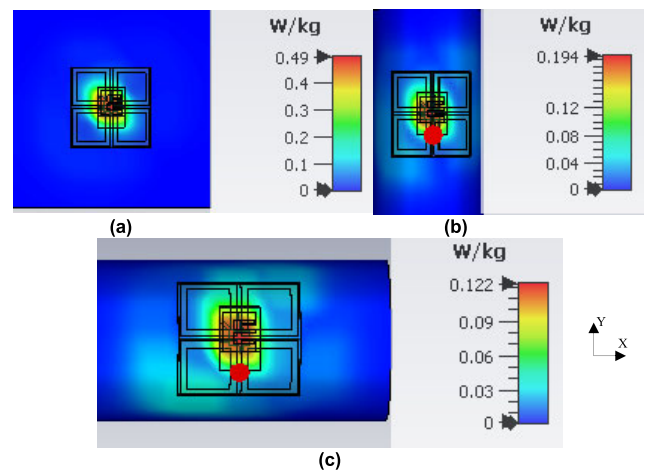


FIGURE 23. SAR levels 4 mm away from the skin over 1 g average: (a) Chest; (b) Bent along y-axis; and (c) Bent along x-axis.

V. CONCLUSION

A wearable symmetrical e-slots antenna over a 2 × 2 EBG array with etched DGS was proposed to operate at 2.4 GHz for Medical Body Area Network applications. The design was numerically and experimentally tested over free space and on the human body. A comparison between the antenna alone and over 2 × 2 EBG arrays with and without etched DGS was carried out. Generally, the results revealed that 2 × 2 EBG with etched DGS had better performance through an increase of bandwidth from 2.09 to 2.86 GHz (32.08%). This widened

**TABLE 4.** Comparison of reported flexible/wearable designs with proposed design.

Ref	Year	No. of unit cells	FBR(dB)	Gain (dBi)	Bandwidth (%)	Overall size (mm <sup>3</sup> )	Substrate type
[13]	2009	3×3	10	6.4	4	120×120×4.3	Fabric
[26]	2013	3×3	8	4.8	18	65.7×65.7×3.3	Viny and Kapton polyimide
[18]	2014	2×2	23	6.2	5.5	62×42×4	Rogers RO3003
[14]	2014	4×4	12	2.5	3.43	100×100×4.5	Fabric
[28]	2015	-	-	3.28	8.1	100×100×3	Textile
[15]	2015	3×3	15.64	N/A	5.08	150×150×4	Fabric
[16]	2016	6×4	20	7	9.52	318×212×7	Fabric
[20]	2016	3×3	12	4.12	1.88	50×50×9.5	Latex
[21]	2017	2×2	12	5.2	11.3	50×50×5	PDMS
[19]	2017	1×2	10	6.88	5	68×38×6.57	RT/duroid 5880
[22]	2018	2×2	13	6.55	8.3	60×60×2.4	Fabric
[17]	2018	3×3	17	7.3	14.7	81×81×4	Fabric
[23]	2019	2×2	13.7	7.5	14.5	60×60×2.4	Fabric
[18]	2019	3×3	-	5.6	-	40×60×5	PDMS
[19]	2019	2×3	-	6.56	14.58	60×60×8.5	PDMS
This work	2020	2×2	15.8	6.45	32.08	60×60×2.4	Fabric

bandwidth made the design highly conformal and robust to deformation and human body loading over antenna with and without  $2 \times 2$  EBG, which showed frequency attenuation and detuning when bent around an arm along the x-axis and y-axis. The etched DGS on EBG ground also showed an improvement of FBR of 15.8 dB, efficiency of 72.3%, and gain of 6.45 dB, respectively. In addition, the etched DGS in EBG ground alleviated SAR by more than 90% compared to symmetrical e-slots antennas alone. Furthermore, the numerical simulation of radiation patterns on the body were greatly affected when the antenna was alone and slightly affected when the antenna was over  $2 \times 2$  EBG with etched DGS compared to free space. Based on this achievement, the proposed symmetrical e-slots antenna over  $2 \times 2$  EBG array with etched DGS is a strong potential candidate for wearable medical applications. Finally, the integration of antenna with EBG-DGS demonstrates a compact fabric design, better FBR, acceptable gain, and wider bandwidth compared to most recently reported configurations listed in Table 4, which are intended for wearable applications.

## REFERENCES

- [1] S. Genovesi, F. Costa, and G. Manara, "Compact antenna for wearable applications," in *Proc. 2nd URSI Atlantic Radio Sci. Meeting (AT-RASC)*, May 2018, pp. 1–3.
- [2] A. Y. I. Ashyap, Z. Z. Abidin, S. H. Dahlan, H. A. Majid, S. K. Yee, G. Saleh, and N. Abdul Malek, "Flexible wearable antenna on electromagnetic band gap using PDMS substrate," *TELKOMNIKA (Telecommun. Comput. Electron. Control)*, vol. 15, no. 3, p. 1454, 2017.
- [3] F. C. Seman, F. Ramadhan, N. S. Ishak, R. Yuwono, Z. Z. Abidin, S. H. Dahlan, S. M. Shah, and A. Y. I. Ashyap, "Performance evaluation of a star-shaped patch antenna on polyimide film under various bending conditions," *Prog. Electromagn. Res. Lett.*, vol. 85, pp. 125–130, Feb. 2019.
- [4] A. Y. I. Ashyap, W. N. N. W. Marzudi, Z. Z. Abidin, S. H. Dahlan, H. A. Majid, and M. R. Kamaruddin, "Antenna incorporated with electromagnetic bandgap (EBG) for wearable application at 2.4 GHz wireless bands," in *Proc. IEEE Asia-Pacific Conf. Appl. Electromagn. (APACE)*, Dec. 2016, pp. 217–221.
- [5] Z. Muhammad, S. M. Shah, Z. Z. Abidin, A. Y. I. Ashyap, S. M. Mustam, and Y. Ma, "CPW-fed wearable antenna at 2.4 GHz ISM band," in *Proc. AIP Conf.*, 2017, vol. 1883, no. 1, Art. no. 020003.
- [6] G.-P. Gao, C. Yang, B. Hu, R.-F. Zhang, and S.-F. Wang, "A wide-bandwidth wearable all-textile PIFA with dual resonance modes for 5 GHz WLAN applications," *IEEE Trans. Antennas Propag.*, vol. 67, no. 6, pp. 4206–4211, Jun. 2019.
- [7] A. Y. I. Ashyap, Z. Z. Abidin, S. H. Dahlan, H. A. Majid, M. R. Kamarudin, and R. A. Abd-Alhameed, "Robust low-profile electromagnetic band-gap-based on textile wearable antennas for medical application," in *Proc. Int. Workshop Antenna Technol., Small Antennas, Innov. Struct., Appl. (iWAT)*, Mar. 2017, pp. 158–161.
- [8] A. Y. I. Ashyap, Z. Z. Abidin, S. H. Dahlan, H. A. Majid, S. M. Shah, M. R. Kamarudin, and A. Alomainy, "Compact and low-profile textile EBG-based antenna for wearable medical applications," *IEEE Antennas Wireless Propag. Lett.*, vol. 16, pp. 2550–2553, 2017.
- [9] P. J. Soh, G. Vandenbosch, F. H. Wee, A. van den Bosch, M. Martinez-Vazquez, and D. Schreurs, "Specific absorption rate (SAR) evaluation of textile antennas," *IEEE Antennas Propag. Mag.*, vol. 57, no. 2, pp. 229–240, Apr. 2015.
- [10] A. Y. I. Ashyap, Z. Z. Abidin, S. H. Dahlan, H. A. Majid, and F. C. Seman, "A compact wearable antenna using EBG for smart-watch applications," in *Proc. Asia-Pacific Microw. Conf. (APMC)*, Nov. 2018, pp. 1477–1479.
- [11] *IEEE Recommended Practice for Measurements and Computations of Radio Frequency Electromagnetic Fields with Respect to Human Exposure to Such Fields, 100 kHz–300 GHz*, Standard IEEE C95.3-2002, 2002.
- [12] *Council Recommendation on Limits for Exposure of the Federal Public to Electromagnetic Fields: 0Hz–300 GHz*, Commission of European Communities, Brussels, Belgium, 1998.
- [13] S. Zhu and R. Langley, "Dual-band wearable textile antenna on an EBG substrate," *IEEE Trans. Antennas Propag.*, vol. 57, no. 4, pp. 926–935, Apr. 2009.
- [14] S. Yan, P. J. Soh, and G. A. E. Vandenbosch, "Low-profile dual-band textile antenna with artificial magnetic conductor plane," *IEEE Trans. Antennas Propag.*, vol. 62, no. 12, pp. 6487–6490, Dec. 2014.
- [15] S. Velan, E. F. Sundarsingh, M. Kanagasabai, A. K. Sarma, C. Raviteja, R. Sivasamy, and J. K. Pakkathillam, "Dual-band EBG integrated monopole antenna deploying fractal geometry for wearable applications," *IEEE Antennas Wireless Propag. Lett.*, vol. 14, pp. 249–252, 2015.
- [16] K. Kamardin, M. K. A. Rahim, P. S. Hall, N. A. Samsuri, T. A. Latef, and M. H. Ullah, "Planar textile antennas with artificial magnetic conductor for body-centric communications," *Appl. Phys. A, Solids Surf.*, vol. 122, no. 4, pp. 1–9, Apr. 2016.

- [17] G.-P. Gao, B. Hu, S.-F. Wang, and C. Yang, "Wearable circular ring slot antenna with EBG structure for wireless body area network," *IEEE Antennas Wireless Propag. Lett.*, vol. 17, no. 3, pp. 434–437, Mar. 2018.
- [18] G. Gao, R. Zhang, C. Yang, H. Meng, W. Geng, and B. Hu, "Microstrip monopole antenna with a novel UC-EBG for 2.4 GHz WBAN applications," *IET Microw., Antennas Propag.*, vol. 13, no. 13, pp. 2319–2323, Oct. 2019.
- [19] G. Gao, S. Wang, R. Zhang, C. Yang, and B. Hu, "Flexible EBG-backed PIFA based on conductive textile and PDMS for wearable applications," *Microw. Opt. Technol. Lett.*, vol. 62, no. 4, pp. 1733–1741, 2020.
- [20] Z. H. Jiang, D. E. Brocker, P. E. Sieber, and D. H. Werner, "A compact, low-profile metasurface-enabled antenna for wearable medical body-area network devices," *IEEE Trans. Antennas Propag.*, vol. 62, no. 8, pp. 4021–4030, Aug. 2014.
- [21] M. A. B. Abbasi, S. S. Nikolaou, M. A. Antoniadis, M. Nikolic Stevanovic, and P. Vryonides, "Compact EBG-backed planar monopole for BAN wearable applications," *IEEE Trans. Antennas Propag.*, vol. 65, no. 2, pp. 453–463, Feb. 2017.
- [22] K. Agarwal, Y.-X. Guo, and B. Salam, "Wearable AMC backed near-endfire antenna for on-body communications on latex substrate," *IEEE Trans. Compon., Packag., Manuf. Technol.*, vol. 6, no. 3, pp. 346–358, Mar. 2016.
- [23] Z. H. Jiang, Z. Cui, T. Yue, Y. Zhu, and D. H. Werner, "Compact, highly efficient, and fully flexible circularly polarized antenna enabled by silver nanowires for wireless body-area networks," *IEEE Trans. Biomed. Circuits Syst.*, vol. 11, no. 4, pp. 920–932, Aug. 2017.
- [24] A. Y. I. Ashyap, Z. Zainal Abidin, S. H. Dahlan, H. A. Majid, M. R. Kamarudin, A. Alomainy, R. A. Abd-Alhameed, J. S. Kosha, and J. M. Noras, "Highly efficient wearable CPW antenna enabled by EBG-FSS structure for medical body area network applications," *IEEE Access*, vol. 6, pp. 77529–77541, 2018.
- [25] A. Y. I. Ashyap, Z. Zainal Abidin, S. H. Dahlan, H. A. Majid, and G. Saleh, "Metamaterial inspired fabric antenna for wearable applications," *Int. J. RF Microw. Comput.-Aided Eng.*, vol. 29, no. 3, Mar. 2019, Art. no. e21640.
- [26] H. R. Raad, A. I. Abbosh, H. M. Al-Rizzo, and D. G. Rucker, "Flexible and compact AMC based antenna for telemedicine applications," *IEEE Trans. Antennas Propag.*, vol. 61, no. 2, pp. 524–531, Feb. 2013.
- [27] A. Y. I. Ashyap, S. H. Dahlan, Z. Z. Abidin, H. A. Majid, F. C. Seman, X. Ngu, and N. A. Cholan, "Flexible antenna with HIS based on PDMS substrate for WBAN applications," in *Proc. IEEE Int. RF Microw. Conf. (RFM)*, Dec. 2018, pp. 69–72.
- [28] J. Tak, Y. Hong, and J. Choi, "Textile antenna with EBG structure for body surface wave enhancement," *Electron. Lett.*, vol. 51, no. 15, pp. 1131–1132, Jul. 2015.
- [29] D. M. N. Elsheikh, H. A. Elsadek, and E. A. Abdallah, "Antenna designs with electromagnetic band gap structures," in *Metamaterial*. Rijeka, Croatia: InTech, 2012.
- [30] *CST Microwave Studio*. Accessed: Oct. 10, 2016. [Online]. Available: <http://www.cst.com>
- [31] A. Y. I. Ashyap, Z. Zainal Abidin, S. H. Dahlan, H. A. Majid, A. M. A. Waddah, M. R. Kamarudin, G. A. Oguntala, R. A. Abd-Alhameed, and J. M. Noras, "Inverted E-Shaped wearable textile antenna for medical applications," *IEEE Access*, vol. 6, pp. 35214–35222, 2018.
- [32] A. Roy, S. Bhunia, D. C. Sarkar, P. P. Sarkar, and S. K. Chowdhury, "Compact multi frequency strip loaded microstrip patch antenna with spurlines," *Int. J. Microw. Wireless Technol.*, vol. 9, no. 5, pp. 1111–1121, Jun. 2017.
- [33] N. C. Karmakar, S. M. Roy, and I. Balbin, "Quasi-static modeling of defected ground structure," *IEEE Trans. Microw. Theory Techn.*, vol. 54, no. 5, pp. 2160–2168, May 2006.
- [34] M. M. Rahman, M. S. Islam, H. Y. Wong, T. Alam, and M. T. Islam, "Performance analysis of a defected ground-structured antenna loaded with stub-slot for 5G communication," *Sensors*, vol. 19, no. 11, p. 2634, 2019.
- [35] D. M. Pozar, *Microwave Engineering*. Hoboken, NJ, USA: Wiley, 2012.
- [36] G. Matthaei, L. Young, and E. Jones, "Design of microwave filters," in *Impedance-Matching Networks, and Coupling Structures*, vol. 2. Menlo Park, CA, USA: Stanford Research Institute, 1963.



**ADEL Y. I. ASHYAP** received the B.Eng., M.Eng., and Ph.D. degrees in electrical engineering from Universiti Tun Hussein Onn Malaysia (UTHM), Parit Raja, Malaysia, in 2012, 2014, and 2019, respectively. He is currently a Postdoctoral Fellow of the Research Center of Applied Electromagnetics, Faculty of Electrical and Electronic Engineering, UTHM. He has authored or coauthored a numbers of journals and proceedings. His research interests include electromagnetic bandgap (EBG), artificial magnetic conductors (AMC) for wireless body area networks (WBAN), and microstrip antennas and small antennas for biomedical devices. He has received the Chancellor Award for his final year project and a number of Gold, Silver, and Bronze medals in international and local competitions.



**SAMSUL HAIMI BIN DAHLAN** received the Ph.D. degree in signal processing and telecommunications from the Universite de Rennes 1, France, in 2012. He has been a Senior Lecturer with the Faculty of Electrical and Electronic Engineering, Universiti Tun Hussein Onn Malaysia (UTHM), since March 2012. He is currently a Principal Researcher with the Research Center for Applied Electromagnetics (EMCenter), UTHM, and was appointed as the Head of the Center, in April 2015. He has authored or coauthored a numbers of journals, including the IEEE TRANSACTION ON ELECTROMAGNETIC COMPATIBILITY and the IEEE ANTENNAS AND WIRELESS PROPAGATION LETTERS. His research interests include optical-microwave generators, focusing systems (dielectric lens and transmitarray's synthesis), computational electromagnetic technique, namely, the BOR-FDTD, and material characterizations. He is supervising a numbers of Ph.D., master's, and bachelor's students and involved in several research projects sponsored by the industry and government agencies.



**ZUHAIIRAH ZAINAL ABIDIN** (Member, IEEE) received the Ph.D. degree from Bradford University, U.K., in 2011. She is a Principal Researcher with the Research Center for Applied Electromagnetics (EMCenter), Universiti Tun Hussein Onn Malaysia. She has authored or coauthored a numbers of journals and proceedings, including the IEEE TRANSACTION ON ANTENNA AND PROPAGATION, IEEE ACCESS, and the IEEE ANTENNAS AND WIRELESS PROPAGATION LETTERS. Her research interests include MIMO antennas, printed microstrip antennas, wearable antennas, and electromagnetic bandgap (EBG) for wireless, mobile, and high-speed digital circuit's applications.



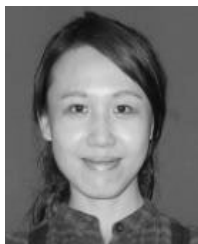
**MUHAMMAD HASHIM DAHRI** received the B.E. degree in telecommunications from the Mehran University of Engineering and Technology (MUET), Pakistan, in 2010, the master's degree by research in electrical engineering from Universiti Tun Hussein Onn Malaysia (UTHM), in 2014, and the Ph.D. degree from the Wireless Communication Centre (WCC), Universiti Teknologi Malaysia (UTM), in 2019. He is currently working as a Postdoctoral Research Fellow of the UTHM. He has authored over 25 research articles in various indexed journals and conference proceedings. His research interests include reflectarray antennas, planar printed antennas, and tunable materials for antenna design.



**HUDA A. MAJID** (Member, IEEE) received the B.Eng. degree in electrical engineering (telecommunication) from Universiti Teknologi Malaysia, in 2007, and the M.Eng. and Ph.D. degrees in electrical engineering from Universiti Teknologi Malaysia, in 2010 and 2013, respectively. He is currently a Lecturer with the Department of Electrical Engineering Technology, Faculty of Engineering Technology, Universiti Tun Hussein Onn Malaysia. He has published over 50 articles in journals and conference papers. His research interests include the areas of design of microstrip antennas, small antennas, reconfigurable antennas, metamaterials structures, metalateral antennas, and millimeter wave antennas.



**MUHAMMAD RAMLEE KAMARUDIN** (Senior Member, IEEE) received the degree (Hons.) majoring in electrical and telecommunication engineering from Universiti Teknologi Malaysia (UTM), Johor Bahru, Malaysia, in 2003, and the M.Sc. degree in communication engineering and the Ph.D. degree in electrical engineering from the University of Birmingham, Birmingham, U.K., in 2004 and 2007, respectively, under the supervision of Emeritus Prof. P. Hall. He has been an Associate Professor with the Faculty of Electrical and Electronic Engineering, Universiti Tun Hussein Onn Malaysia, since May 2019. Prior to this appointment, he was a Senior Lecturer with the Centre for Electronic Warfare, Information and Cyber, Cranfield Defense and Security, Cranfield University, U.K., and an Associate Professor with the Wireless Communication Centre, UTM. He holds a SCOPUS H-Index of 23 with over 2000 citations. He has authored a book chapter of a book entitled *Antennas and Propagation for Body-Centric Wireless Communications* and has published over 240 technical articles in leading journals and international proceedings, including the IEEE TRANSACTION ON ANTENNAS AND PROPAGATION, the IEEE ANTENNAS AND WIRELESS PROPAGATION LETTERS, the *IEEE Antenna Magazine*, IEEE ACCESS, the *International Journal of Antennas and Propagation*, *Progress in Electromagnetic Research*, *Microwave and Optical Technology Letters*, and *Electronics Letters*. His research interests include antenna design for 5G/6G, MIMO antennas, array antenna for beam-forming and beam steering, wireless on-body communications, in-body communications (implantable antenna), RF and microwave communication systems, and antenna diversity. He is a member of the IET, an Executive Member of Antenna and Propagation Society, Malaysia Chapter, and a member of the IEEE Antennas and Propagation Society, the IEEE Communication Society, the IEEE Microwave Theory and Techniques Society, and the IEEE Electromagnetic Compatibility Society, an Associate Editor of *Electronics Letters* and *IET Microwaves, Antennas and Propagation*, and an Academic Editor of the *International Journal of Antennas and Propagation*.



**SEE KHEE YEE** received the Ph.D. degree from the Faculty of Electrical and Electronic Engineering, Universiti Tun Hussein Onn Malaysia (UTHM), in 2015. She is a Principal Researcher with the Research Center for Applied Electromagnetic and a Lecturer with the Department of Communication Engineering, Faculty of Electrical and Electronic Engineering, UTHM. Her research interests include shielding effectiveness, and dielectric measurement techniques and its applications in sensing.



**MOHD HAIZAL JAMALUDDIN** (Member, IEEE) received the bachelor's and master's degrees in electrical engineering from Universiti Teknologi Malaysia (UTM), Malaysia, in 2003 and 2006, respectively, and the Ph.D. degree in signal processing and telecommunications from the Université de Rennes 1, France, in 2009, with a focus on microwave communication systems and specially antennas such as dielectric resonator and reflectarray and dielectric dome antennas. He is currently an Associate Professor with the Wireless Communication Centre, School of Electrical Engineering, UTM. He has published more than 100 articles in reputed indexed journals and conference proceedings. His research interests include dielectric resonator antennas, printed microstrip antennas, MIMO antennas, and DRA reflectarray antennas.



**AKRAM ALOMAINY** (Senior Member, IEEE) received the M.Eng. degree in communication engineering and the Ph.D. degree in electrical and electronic engineering (specialized in antennas and radio propagation) from the Queen Mary University of London (QMUL), London, U.K., in 2003 and 2007, respectively. In 2007, he joined the School of Electronic Engineering and Computer Science, QMUL, where he is currently an Associate Professor (Senior Lecturer) with the Antennas and Electromagnetics Research Group. He is a member of the Centre for Intelligent Sensing, Institute of Bioengineering, QMUL. He has authored or coauthored a book, five book chapters, and more than 220 technical articles (over 3900 citations and H-index 29) in leading journals and peer-reviewed conferences. His current research interests include small and compact antennas for wireless body area networks, radio propagation characterization and modeling, antenna interactions with human body, computational electromagnetics, advanced antenna enhancement techniques for mobile and personal wireless communications, and advanced algorithms for smart and intelligent antenna and cognitive radio systems. He is a member of the IET, a Fellow of the Higher Education Academy, U.K., and also a College Member of the Engineering and Physical Sciences Research (EPSRC) Council, U.K., and its ICT prioritization panels. He was a recipient of the Isambard Brunel Kingdom Award, in 2011, for being an outstanding young science and engineering communicator. He was selected to deliver a TEDx talk about the science of electromagnetics and also participated in many public engagement initiatives and festivals. He is also a reviewer for many funding agencies around the world including Expert Swiss National Science Foundation Research, the EPSRC, and the Medical Research Council, U.K. He was an Elected Member of the International Union of Radio Science (URSI), U.K., a panel to represent the U.K. interests of URSI Commission B, from September 1 2014 to Aug 31 2017. He has managed to secure various research projects funded by research councils, charities, and industrial partners on projects ranging from fundamental electromagnetic to wearable technologies. He is the Lead of wearable creativity research with the QMUL, and he has been invited to participate at the Wearable Technology Show 2015 with Innovate U.K., in 2015, and in the recent Wearable Challenge organized by Innovate U.K. IC Tomorrow as a Leading Challenge Partner to support SMEs and industrial innovation.



**QAMMER H. ABBASI** (Senior Member, IEEE) received the B.Sc. and M.Sc. degrees in electronics and telecommunication engineering from the University of Engineering and Technology (UET), Lahore, Pakistan, and the Ph.D. degree in electronic and electrical engineering from the Queen Mary University of London (QMUL), U.K., in 2012. In 2012, he was a Postdoctoral Research Assistant with the Antenna and electromagnetics Group, QMUL. He is currently a Lecturer (Assistant Professor) with the School of Engineering, University of Glasgow, U.K. He has contributed over 250 leading international technical journal and peer reviewed conference papers, and eight books. His research interests include nano communication, the Internet of Things, RF design and radio propagation, biomedical applications of millimeter and terahertz communication, wearable and flexible sensors, compact antenna design, antenna interaction with human body, implants, body centric wireless communication issues, wireless body sensor networks, non-invasive health care solutions, and physical layer security for wearable/implant communication. He is a member of the IET and a Committee Member of IET Antenna & Propagation

and healthcare network. He has been a member of the technical program committees of several IEEE flagship conferences. He contributed in organizing several IEEE conferences, workshops, and special sessions in addition to the European school of antenna course. He received several recognitions for his research, which includes appearance in BBC, STV, dawnnews, local and international newspapers, cover of MDPI journals, most downloaded articles, U.K. exceptional talent endorsement by the Royal Academy of Engineering, the National Talent Pool Award by Pakistan, the International Young Scientist Award by NSFC China, the URSI Young Scientist Award, the National Interest Waiver by USA, four best paper awards, and best representative image of an outcome by QNRF. He was the Chair of IEEE Young Professional Affinity Group. He is an Associate Editor of the IEEE JOURNAL OF ELECTROMAGNETICS, RF, and MICROWAVES IN MEDICINE AND BIOLOGY, the IEEE SENSORS JOURNAL, the IEEE OPEN ACCESS ANTENNA AND PROPAGATION, and IEEE ACCESS journal and acted as a Guest Editor for numerous special issues in top notch journals. He was a Technical Reviewer of several IEEE and top notch journals, including the TPC Chair of Fourth International UCET Conference, in 2019.

• • •